A Small-Angle Neutron Scattering Study of Surfactant Aggregates Formed in Aqueous Mixtures of Sodium Dodecyl Sulfate and Didodecyldimethylammonium Bromide

Magnus Bergström*

Department of Chemistry, Surface Chemistry, Royal Institute of Technology, SE-100 44 Stockholm, Sweden

Jan Skov Pedersen

Condensed Matter Physics and Chemistry Department, Risø National Laboratory, DK-4000 Roskilde, Denmark

Received: October 14, 1999; In Final Form: January 20, 2000

The structure of aggregates formed in aqueous mixtures of a single-chain anionic surfactant, sodium dodecyl sulfate (SDS), and a double-chain cationic surfactant, didodecyldimethylammonium bromide (DDAB), has been investigated at 38 °C using small-angle neutron scattering (SANS). Several overall surfactant concentrations [SDS] + [DDAB] between 0.1 and 5 wt % were measured at the two SDS-rich compositions [SDS]:[DDAB] = 90:10 and 95:5. Samples with a concentration above about [SDS] + [DDAB] = 1 wt % at [SDS]:[DDAB] = 95:5 contained only somewhat elongated tablet-shaped micelles (triaxial ellipsoids) with typical values of the half-axes a (related to the thickness) = 14 Å, b (related to the width) = 23 Å, and c (related to the length) = 27 Å. When a sample at [SDS]:[DDAB] = 95:5 is diluted below about [SDS] + [DDAB] = 1 wt %, an increasing amount of small unilamellar vesicles forms, and in the samples below about 0.2 wt %, only vesicles are observed. The average radius of the vesicles $\langle R \rangle$ increases from about 90 Å at 0.3 wt % to 110 Å at 0.1 wt %. The transition from micelles to vesicles with decreasing surfactant concentration was also observed in the samples at [SDS]:[DDAB] = 90:10 in which, however, an additional amount of bilayer sheets was seen to be always present. Compared with the micelles at [SDS]:[DDAB] = 95:5, the micelles formed at [SDS]:[DDAB] = 90:10 were considerably longer ($c \approx 40$ Å), but with similar cross section dimensions, and the vesicles formed were seen to be somewhat larger than the corresponding aggregates at 95:5. The relative standard deviation $\sigma_R/\langle R \rangle$ of the (number-weighted) vesicle size distributions was in the range $0.2 < \sigma_R/\langle R \rangle < 0.3$.

Introduction

During the past decade a variety of different microstructures have been observed in various electron microscopy studies of aqueous mixtures of two oppositely charged surfactants including small globular as well as large wormlike micelles, rather small unilamellar vesicles, and large lamellar sheets.[1−5] Particular interest has been focused on the spontaneous formation of geometrically closed bilayer vesicles, since mixtures of an anionic and a cationic surfactant appear to be one of the rare examples of systems in which thermodynamically equilibrated vesicles may form.[1]

In recent small-angle neutron scattering (SANS) investigations of aqueous mixtures of an anionic (sodium dodecyl sulfate, SDS) and a cationic surfactant (dodecyltrimethylammonium bromide, DTAB), i.e. two single-chain surfactants with identical C_{12} hydrocarbon parts, in pure D_2O as well as in [NaBr] = 0.1 M at 40 °C, different surfactant aggregate structures were observed, depending on the concentrations of the surfactants [SDS] and [DTAB], respectively.[6−9] In samples containing either pure SDS or DTAB, rather small oblate or disk-shaped micelles were seen to form,[10] and as an increasing amount of the oppositely charged surfactant was admixed, the micelles were seen to grow in size into elongated tablet-shaped or ribbonlike micelles.[7,8] As the equimolar composition was further approached, a transition from micelles to either geometrically closed bilayer shells (vesicles) or stacks of lamellar sheets eventually occurred.[9]

The magnitudes of the free monomer concentrations of two surfactants in a mixture of an anionic and a cationic surfactant where either of the surfactant is in excess are very different. The reason for this is that electrostatics contribute to the chemical potential of the aggregated surfactant in excess but not to the surfactant in deficit. Since the chemical potentials of free surfactants, $\mu_{ex}^{free} \propto \ln c_{ex}^{free}$ and $\mu_{def}^{free} \propto \ln c_{def}^{free}$, (approximately) equals the corresponding quantities of aggregated surfactant, the concentration of free surfactant in excess must be much larger than the free monomer concentration of the surfactant in deficit c_{ex}^{free}.[11] As a result, the fraction of the surfactant in deficit *in the aggregates* has been observed to increase with decreasing overall surfactant concentration at a fixed overall surfactant ratio at concentrations close to the critical micelle concentration.[12] Consequently, we observed a growth of mixed SDS/DTAB micelles with decreasing surface charge density during a dilution path below about 1 wt % surfactant as well as, eventually, the spontaneous formation of vesicles.[8,9] This change in aggregate composition with overall surfactant concentration as a result of a free monomer effect is expected to be enhanced for SDS-rich systems when the single-chain cationic surfactant DTAB is exchanged with its water insoluble double-chain counterpart, didodecyldimethylammonium bromide (DDAB).

* Address for correspondence: Institute for Surface Chemistry, Box 5607, SE-114 86 Stockholm, Sweden. Tel: +46 8 790 99 05. Fax: +46 8 20 89 98. E-mail: magnus.bergstrom@surfchem.kth.se.

10.1021/jp993666s CCC: $19.00
Published on Web 04/05/2000

Mixtures of SDS and DDAB have been measured by Marques et al. at 40 °C[13] using dynamic light scattering (DLS) and various NMR (nuclear magnetic resonance) techniques and, more recently, at 25 °C[14] using, in addition to DLS and NMR, cryo-transmission electron microscopy (CRYO-TEM) and light microscopy. From the detailed study at 25 °C it was found that small spheroidal micelles coexisted with rather small unilamellar vesicles above about $X \equiv [SDS]/([SDS] + [DDAB]) = 0.94$. Between $X = 0.75$ and 0.94, the small micelles were seen to be replaced by larger disklike aggregates, and in the interval $0.66 < X < 0.75$, only vesicles considerably larger than at lower values of X could be observed. Above about 0.5−2 wt % surfactant the isotropic vesicle/micelle solutions were seen to coexist with a lamellar phase. Close to equimolar composition and at DDAB-rich surfactant mixtures ($X < 0.5$)[15] the solutions appeared to be more complicated.

The present work consists of a SANS study of SDS-rich ($X = 0.90$ and 0.95) surfactant aggregates formed in mixtures of SDS and DDAB, i.e., an anionic single-chain and a cationic double-chain surfactant with identical aliphatic C_{12} chains, in dilute samples of D_2O ($c_{surf}^{tot} \equiv [SDS] + [DDAB] < 5$ wt %) at 38 °C. To enable a quantitative analysis of our SANS data we have chosen to study the comparatively simple systems in which SDS is in significant excess rather than the more complicated gel-like solutions near equimolar composition and at an excess amount of DDAB.

Materials and Methods

Materials. Sodium dodecyl sulfate (SDS) (>99% purity) was obtained from Merck, whereas 99% didodecyldimethylammonium bromide (DDAB) and D_2O with 99.9 atom % D were obtained from Aldrich Chemical Co. The chemicals were used without further purification.

Sample Preparation. Stock solutions containing SDS or DDAB in pure D_2O were prepared by simply mixing either of the surfactants with D_2O to yield an overall surfactant concentration of 5.0 wt % SDS (about 191 mM) and the same molar concentration of DDAB (about 8.0 wt %). D_2O was chosen in order to minimize the incoherent background from hydrogen and obtain a high scattering contrast. The stock solutions were mixed in the appropriate proportions to yield the overall molar compositions $X \equiv [SDS]/([SDS] + [DDAB]) = 0.90$ and 0.95, respectively. The final samples were then obtained by means of diluting the two solutions at $X = 0.90$ and 0.95 to overall surfactant concentrations with molar concentrations identical to those for 2.5, 1.5, 1.0, 0.70, 0.50, 0.30, 0.20, 0.15, and 0.10 wt % pure SDS. Each sample were equilibrated at least 48 h at 38 °C before measured.

Methods. The small-angle neutron scattering (SANS) experiments were performed at the SANS instrument at the DR3 reactor at Risø National Laboratory, Roskilde, Denmark.[16] A range of scattering vectors q from 0.004 to 0.5 Å^{-1} was covered by four combinations of neutron wavelength (3 and 10 Å) and sample-to-detector distances (1−6 m). The different settings overlap each other in a wide regime of q values, and the overlaps between different settings were optimized by three scale factors obtained by fitting to the data. The setting with 3 Å neutron wavelength and 3 m sample-to-detector distance was used as the reference setting for the absolute scale. The wavelength resolution was 18% (full width at half-maximum value).

The samples were kept in quartz cells (Hellma) with a path length of either 2 or 10 mm, depending on concentration. The raw spectra were corrected for background from the solvent, sample cell, and other sources by conventional procedures.[17] The two-dimensional isotropic scattering spectra were azimuthally averaged, converted to an absolute scale, and corrected for detector efficiency by dividing by the incoherent scattering spectra of pure water measured in a 1 mm cell.[18] The scattering intensity was furthermore normalized by dividing with the concentrations in g/mL of solute (SDS + DDAB).

The average excess scattering length density per unit mass of solute, $\Delta\rho_m$, was calculated using the appropriate molecular volumes and weights of the surfactant monomers ($\Delta\rho_m = -5.14 \times 10^{10}$ cm/g for SDS and $\Delta\rho_m = -7.01 \times 10^{10}$ cm/g for DDAB).[19] The molecular weight of SDS is 288.38 g/mol and of DDAB, 462.65 g/mol, and the molecular volumes are 410 Å^3 (SDS) and 810 Å^3 (DDAB).

Throughout the data analyses corrections were made for instrumental smearing.[16,20] For each instrumental setting the ideal model scattering curves were smeared by the appropriate resolution function when the model scattering intensity was compared with the measured one by means of least-squares methods. The parameters in the model were optimized by means of conventional least-squares analysis, and the errors of the parameters were calculated by conventional methods.[21,22]

Data Analyses

The excess scattering length density relative to a solvent of D_2O of an outer layer of sulfate headgroups mixed with a certain number of D_2O molecules is negligible as compared to the inner core of hydrocarbon chains.[10] Likewise, the largely hydrophobic TAB^+ headgroups of DTAB, which are not expected to mix with the surrounding water molecules, have virtually identical excess scattering length density as the hydrocarbon part. As a consequence, we have been able to fit the scattering data for various surfactant aggregates formed by mixtures of SDS and DTAB using various one-shell models for the aggregate structure where, accordingly, the thickness of the aggregates corresponds to the hydrocarbon core.[7,8,9] The largely hydrophobic headgroup of DDAB is similar to that for DTAB, and hence, we have been able to use one-shell rather than two-shell models also in the analyses of aggregates formed by SDS and DDAB. Below follows an outline of the various models used in our analyses of the SANS data. Although it was necessary to use rather complicated models (micelles coexisting with vesicles and/or planar bilayers) when analyzing some of the samples, we have been careful not to include more fit parameters than needed in order to obtain agreement with the SANS data.

The scattering cross section per unit mass of solute for a sample of monodisperse anisotropic micelles can be written as follows

$$\frac{d\sigma(q)}{d\Omega} = \Delta\rho_m^2 M \langle F^2(q)\rangle_0 \left[1 + \frac{\langle F(q)\rangle_0^2}{\langle F^2(q)\rangle_0}(S(q) - 1)\right] \quad (1)$$

where q is the scattering vector, $\Delta\rho_m$ is the difference in scattering length per unit mass solute between particles and solvent, and M is the molar mass of a particle. To account for electrostatic as well as excluded volume interactions between the comparatively small micelles, we have used the decoupling approximation,[23] valid for particles with a small anisotropy, together with a structure factor, $S(q)$. The latter was derived by Hayter and Penfold[24] from the Ornstein−Zernike equation in the rescaled mean spherical approximation (RMSA),[25] with a soft repulsive potential between two macroions surrounded by a diffuse double layer of counterions as calculated from the Poisson−Boltzmann theory. The hard-sphere radius of the micelles were set equal to the radius of the volume equivalent

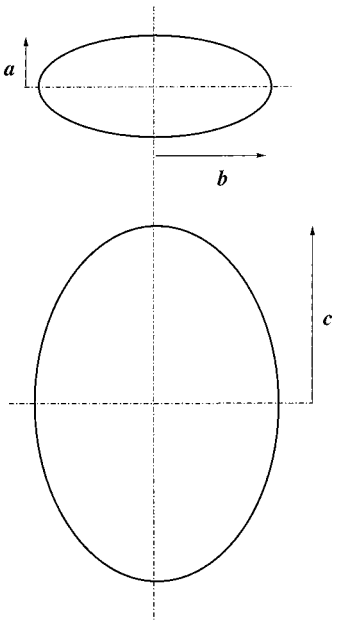

Figure 1. Schematic representation of a model for triaxial ellipsoids with half-axes a (related to the thickness) < b (related to the width) < c (related to the length) used for fitting the SANS data of samples containing micelles.

sphere, and the free monomer concentration, as obtained from the absolute intensities (cf. further below), was subtracted from the overall surfactant concentration as the volume fraction of micelles was calculated. We may note that the main purpose of our study is to obtain the geometrical structure of the various aggregates, and hence, we have aimed at eliminating the structure factor effects by the simple, but less reliable, RMSA approximation, which is easier to use than more elaborated approaches.

The orientational averaged form factor for a triaxial ellipsoid with half-axes $a < b < c$ (cf. Figure 1) equals[26]

$$\langle F^2(q)\rangle_0 = \frac{2}{\pi}\int_0^{\pi/2}\int_0^{\pi/2} F^2[q,r(a,b,c,\phi,\theta)]\sin\phi \, d\phi \, d\theta \quad (2)$$

where the amplitude is

$$F(q,r) = \frac{3[\sin(qr) - qr\cos(qr)]}{(qr)^3} \quad (3)$$

and

$$r(a,b,c,\phi,\theta) = \sqrt{(a^2\sin^2\theta + b^2\cos^2\theta)\sin^2\phi + c^2\cos^2\phi} \quad (4)$$

$\langle F(q)\rangle_0$ is obtained analogously by integration over the amplitude.

The scattering cross section for polydisperse unilamellar vesicles with a bilayer volume V and with radii R much larger than half the bilayer thickness ξ can be written as follows

$$\frac{d\rho(q)}{d\Omega} = \Delta\rho_m^2\langle A\rangle_{HW}\Gamma_m P_{bil}(q)\langle V^2 P_{shell}(q)\rangle[1 + \beta(q)(S(q) - 1)] \quad (5)$$

where the form factor has been separated into two contributions. One accounts for the bilayer cross section

$$P_{bil}(q) = \left(\frac{\sin(q\xi)}{q\xi}\right)^2 \quad (6)$$

and the other for a collection of polydisperse infinitely thin spherical shells with a number-weighted size distribution $N(R)$[22]

$$\langle V^2 P_{shell}(q)\rangle = \int N(R)\, V^2(R)\, F^2(q,R)\, dR \quad (7)$$

where

$$F(q,R) = \frac{\sin(qR)}{qR} \quad (8)$$

$\langle A\rangle_w$ is the weight-averaged area and Γ_m the mass per unit area of the vesicles.

The computing times in the data analyses were considerably reduced by separating the vesicle form factor into a cross section and shell part. Since identical results for the smallest vesicles found ($R \approx 7\xi$) were obtained using eq 5 and the corresponding expression with an exact form factor for spherical shells with thickness 2ξ, we may conclude that eq 5 is a sufficiently accurate approximation for the samples we have investigated.

We have assumed the number-weighted vesicle size distribution to be described by a Schultz distribution with respect to R^2, i.e.

$$N(R) = \frac{2R^{2z+1}}{z!}\left(\frac{z+1}{\langle R^2\rangle}\right)^{z+1} e^{-R^2(z+1)/\langle R^2\rangle} \quad (9)$$

The relative standard deviation of the distribution with respect to R is equal to

$$\frac{\sigma_R}{\langle R\rangle} = \sqrt{\frac{2(\alpha+1)}{\alpha^2}\left[\frac{\Gamma((\alpha+1)/2)}{\Gamma(\alpha/2)}\right]^2 - 1} \quad (10)$$

where $\alpha = 2z + 1$ and $\Gamma(x)$ is the gamma function. When necessary, the RMSA structure factor $S(q)$, accounting for the electrostatic double layer interactions, was invoked using the decoupling approximation, according to which $\beta(q)$ is defined as

$$\beta(q) = \frac{[\int N(R)\, V(R)\, F(q,R)\, dR]^2}{\int N(R)\, V^2(R)\, F^2(q,R)\, dR} \quad (11)$$

The scattering cross section for a sample where micelles and vesicles coexist may be written as a sum of contributions from the micelles and the vesicles, respectively, i.e.

$$\frac{d\sigma(q)}{d\Omega} = I_{ves} + I_{mic} = \Delta\rho_m^2[f_{ves}\langle A\rangle_w\Gamma_m P_{bil}(q)\langle V^2 P_{shell}(q)\rangle[1 + \beta(q)(S(q) - 1)] + (1 - f_{ves})M_{mic}\langle F^2(q)\rangle_0] \quad (12)$$

where f_{ves} is the mass fraction of vesicles coexisting with micelles of identical composition. Interactions could only be determined for the predominating surfactant aggregate (vesicles in eq 12) and, accordingly, a structure factor was not included for the aggregate in deficit. The exception is the isotropic phase at $X = 0.90$ and $c_{surf}^{tot} = 5$ wt % (the sample separates into two phases, cf. further below), in the model fit of which a RMSA structure factor was used for the micelles. However, as it is difficult to accurately determine the appropriate volume fraction of vesicles in this particularly complicated sample, we have simply used a vesicle structure factor for excluded volume interactions where the excluded volume was treated as an

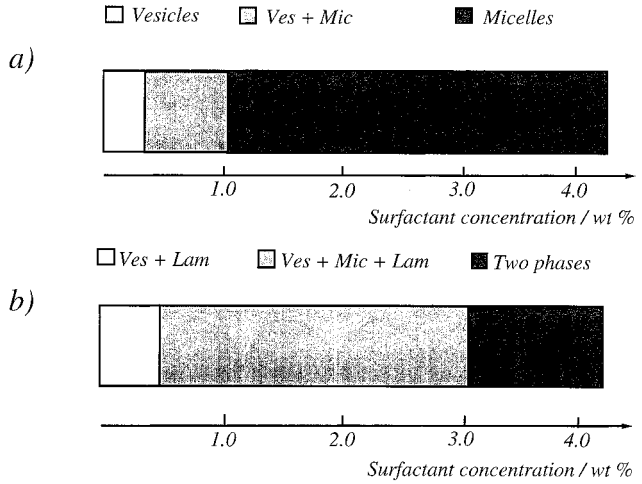

Figure 2. Diagrams showing the various microstructures formed at different surfactant concentrations $c_{surf}^{tot} \equiv$ [SDS] + [DDAB] at surfactant compositions (a) [SDS]:[DDAB] = 95:5 and (b) [SDS]:[DDAB] = 90:10. At higher surfactant concentrations for [SDS]:[DDAB] = 90:10 the sample is separated into an isotropic solution containing micelles and vesicles (cf. Figure 5) and a lamellar phase.

effective fit parameter. The structure factor appeared to be sufficiently good for our purpose to obtain reasonable agreement between model fit and data in the very low q regime (cf. Figure 5 further below).

The data of the samples at $X = 0.90$ could only be fitted by assuming a certain amount of rather large flat bilayers to coexist with the micelles and the vesicles. The corresponding scattering cross section is

$$\frac{d\sigma(q)}{d\Omega} = I_{ves} + I_{mic} + I_{lam} = \Delta\rho_m^2[f_{ves}\langle A\rangle_w\Gamma_m P_{bil}(q)\langle V^2 P_{shell}(q)\rangle[1 + \beta(q)(S(q) - 1)] + f_{mic}M_{mic}\langle F^2(q)\rangle_0 + (1 - f_{ves} - f_{mic})A_{disk}\Gamma_m P_{bil}(q)P_{disk}(q)] \quad (13)$$

where $A_{disk} = \pi R_b^2$ and

$$P_{disk}(q) = \frac{2[1 - B_1(2qR_b)/qR_b]}{(qR_b)^2} \quad (14)$$

is the form factor of an infinitely thin circular disk with radius R_b. When the lamellar fragments were too large for their disk radius to be determined from the range of scattering vectors obtained with our SANS equipment, $A_{disk}P_{disk}$ was set equal to $2\pi/q^2$.

Results and Discussion

An overview of the various structures we have found at $X = 0.90$ and 0.95, respectively, is given in two diagrams in Figure 2 and the detailed results of our SANS data analyses are given in Table 1. Whereas only micelles and/or small unilamellar vesicles were observed in the various samples at $X = 0.95$, agreement with scattering data at $X = 0.90$ could only be obtained by assuming a certain amount of flat lamellar sheets to be present in the samples together with the micelles and/or the vesicles. Above about $c_{surf}^{tot} = 1.0$ wt % at $X = 0.95$, only micelles are observed in the samples. The corresponding data were best fitted with a model for triaxial ellipsoids (cf. Figure 1), and hence, the micelles were seen to be shaped as somewhat elongated tablets rather than strictly oblate ellipsoids of revolutions as the micelles of similar size formed in mixtures of SDS and DTAB.[8] This observation agrees qualitatively with a recent theory for tablet-shaped micelles based on the curvature free energy of the end caps.[27,8]

In the theory[27] it is shown that the structure of the micelles is largely determined by the first- and second-order constants k_1 and k_2 in an expansion of the free energy per unit area of the toroidal end caps $\gamma_t = \gamma_c + k_1/r + k_2/r^2$, where γ_c is the free energy per unit area of a straight cylinder and r is the radius of curvature of the toroidal ends at the mid-plane of a tablet-shaped micelle. In accordance, tablet-shaped micelles rather than cylindrical rods may form as a result of a more favorable lower curvature of the ends of the micelle. It appears that k_2 largely determines the length-to-width ratio of the tablet-shaped micelles (low values of k_2 favor more elongated micelles) whereas the overall size of the micelles is mainly determined by k_1. The mixing of two surfactants with identical hydrocarbon parts gives rise to an always negative term to the electrostatic contribution to k_2, but does not influence k_1 at all, and the magnitude of this contribution increases with increasing difference in charge number between the two surfactants (=2 for a mixture of a monovalent anionic and a monovalent cationic surfactant). This contribution to k_2 is a result of the fact that the curvature dependent surfactant composition is different in the various geometrical parts of the micelle, and hence, k_2 is brought down as electric charge (that is, the surfactant in excess) accumulates in the most curved parts of the micelles.

When considering mixtures of two surfactants with hydrocarbon tails of different volumes, an additional term to the electrostatic contribution to k_2, but none to the corresponding expression for k_1, appears that is negative if the surfactant that carries the charge, i.e., the surfactant in excess, has the smaller tail, but is otherwise positive. Hence, the larger asymmetry between a single-chain surfactant and an oppositely charged double-chain surfactant when the former is in excess makes it even more preferable for the single chain surfactant to be located in the highly curved end caps and, as a result, the micelles formed in an SDS-rich mixture of SDS and DDAB are expected to be more elongated than the corresponding micelles formed in mixtures of SDS and the single chain surfactant DTAB.

The half-axes related to the thickness and width of the micelles were seen to be rather constant ($a \approx 14$ Å and $b \approx 23$ Å) with respect to the overall surfactant concentration at $X = 0.95$. The half-axis related to the length of the elongated micelles is seen to slightly increase with c_{surf}^{tot} in the interval 1 wt % < c_{surf}^{tot} < 5 wt % from $c = 24$ to 32 Å as the entropy of mixing aggregates and solvent (the free energy contribution of which favors small aggregates) decreases. Typical values of the error bars of the dimensions a, b, and c, respectively, in samples where only tablet-shaped micelles exist are $\sigma(a) = \pm 0.2$ Å and $\sigma(b) = \pm 0.5$ Å and $\sigma(c) = \pm 0.5$ Å.

The concentration of free SDS monomers largely exceeds the corresponding quantity for DDAB at the surfactant compositions we have investigated. Hence, the compositions in the micelles change so that the fraction of DDAB increases when the samples are diluted at a fixed overall composition X (cf. above in the Introduction). As a result, the length of the micelles slightly increases below about $c_{surf}^{tot} = 1$ wt % at $X = 0.95$. Moreover, due to the free monomer effect, a significantly increasing fraction of vesicles coexist with the micelles upon further diluting the samples and, at $c_{surf}^{tot} = 0.31$ wt %, 67% of the mass of the aggregated surfactant is incorporated in vesicles and 23% is in the micelles. The samples at $c_{surf}^{tot} = 0.2$ wt %

TABLE 1: Results of SANS Data Analyses of Samples where Various Aggregates Form in Mixtures of SDS and DDAB at 38 °C in D_2O[a]

[SDS]:[DDAB]	0.10 wt %	0.15 wt %	0.20 wt %	0.31 wt %	0.51 wt %
95:05	vesicles $\langle R\rangle = 109$ $\sigma_R/\langle R\rangle = 0.22$ $\xi = 14.1$ $c_{free} = 3.2$ mM $x = 0.69$	vesicles $\langle R\rangle = 93.4$ $\sigma_R/\langle R\rangle = 0.24$ $\xi = 12.6$ $c_{free} = 4.6$ mM $x = 0.74$	vesicles $\langle R\rangle = 88.0$ $\sigma_R/\langle R\rangle = 0.24$ $\xi = 11.9$ $z_{eff}/z_{id} = 0.02$ $c_{free} = 6.0$ mM $x = 0.74$	67% vesicles $\langle R\rangle = 89.8$ $\sigma_R/\langle R\rangle = 0.21$ $\xi = 14.9$ + 23% micelles $a = 11.8$ $b = 21.4$ $c = 27.9$ $c_{free} = 6.8$ mM $x = 0.88$	micelles $a = 13.7$ $b = 23.2$ $c = 27.7$ $z_{eff}/z_{id} = 0.16$ + <1% vesicles $c_{free} = 7.1$ mM $x = 0.92$
[SDS]:[DDAB]	0.72 wt %	1.0 wt %	1.5 wt %	2.6 wt %	5.2 wt %
95:05	micelles $a = 13.9$ $b = 22.4$ $c = 26.9$ $z_{eff}/z_{id} = 0.19$ + <1% vesicles $c_{free} = 6.9$ mM $x = 0.93$	micelles $a = 13.2$ $b = 22.0$ $c = 23.8$ $z_{eff}/z_{id} = 0.23$ + <1% vesicles $c_{free} = 6.5$ mM $x = 0.94$	micelles $a = 14.1$ $b = 22.8$ $c = 27.0$ $z_{eff}/z_{id} = 0.20$ $c_{free} = 10$ mM $x = 0.94$	micelles $a = 14.3$ $b = 24.0$ $c = 27.6$ $z_{eff}/z_{id} = 0.26$ $c_{free} = 17$ mM $x = 0.94$	micelles $a = 14.6$ $b = 23.9$ $c = 32.3$ $z_{eff}/z_{id} = 0.32$ $c_{free} = 30$ mM $x = 0.94$
[SDS]:[DDAB]	0.11 wt %	0.16 wt %	0.21 wt %	0.32 wt %	0.53 wt %
90:10	49% vesicles $\langle R\rangle = 117$ $\sigma_R/\langle R\rangle = 0.25$ $\xi = 14.4$ + 51% bilayers $R_b = 468$ $c_{free} = 2.6$ mM $x = 0.69$	51% vesicles $\langle R\rangle = 96.9$ $\sigma_R/\langle R\rangle = 0.29$ $\xi = 13.0$ + 49% bilayers $R_b = 402$ $c_{free} = 3.5$ mM $x = 0.71$	43% vesicles $\langle R\rangle = 94.4$ $\sigma_R/\langle R\rangle = 0.26$ $\xi = 12.5$ + 57% bilayers $R_b = 394$ $c_{free} = 4.8$ mM $x = 0.73$	48% vesicles $\langle R\rangle = 78.7$ $\sigma_R/\langle R\rangle = 0.24$ $\xi = 11.9$ + 52% bilayers $c_{free} = 6.5$ mM $x = 0.77$	58% micelles $a = 12.7$ $b = 22.7$ $c = 27.2$ + 4% vesicles $\langle R\rangle = 90.5$ $\sigma_R/\langle R\rangle = 0.11$ $\xi = 12.7$ + 38% bilayers $c_{free} = 5.6$ mM $x = 0.86$
[SDS]:[DDAB]	0.74 wt %	1.1 wt %	1.6 wt %	2.6 wt %	5.3 wt %
90:10	53% micelles $a = 13.0$ $b = 26.0$ $c = 27.7$ + 6% vesicles $\langle R\rangle = 193$ $\sigma_R/\langle R\rangle = 0.06$ $\xi = 13.7$ + 41% bilayers $c_{free} = 6.8$ mM $x = 0.87$	62% micelles $a = 14.1$ $b = 22.3$ $c = 33.7$ + 13% vesicles $\langle R\rangle = 170$ $\sigma_R/\langle R\rangle = 0.23$ $\xi = 15.5$ + 25% bilayers $c_{free} = 9.7$ mM $x = 0.87$	95% micelles $a = 16.9$ $b = 20.9$ $c = 40.2$ $z_{eff}/z_{id} = 0.20$ + 3% vesicles $\langle R\rangle = 157$ $\sigma_R/\langle R\rangle = 0.19$ + 2% bilayers $c_{free} = 17$ mM $x = 0.86$	96% micelles $a = 16.1$ $b = 23.3$ $c = 41.1$ $z_{eff}/z_{id} = 0.19$ + 2.5% vesicles $\langle R\rangle = 169$ $\sigma_R/\langle R\rangle = 0.18$ + 1.5% bilayers $c_{free} = 27$ mM $x = 0.86$	isotropic phase 80% micelles $a = 14.8$ $b = 27.1$ $c = 56.7$ $z_{eff}/z_{id} = 0.07$ + 20% vesicles $\langle R\rangle = 202$ $\sigma_R/\langle R\rangle = 0.14$ $\xi = 16.8$ + lamellar phase

[a] The data of samples at [SDS]:[DDAB] = 95:5 were fitted with either a model for monodisperse tri-axial ellipsoids with half-axes a (related to the thickness) < b (related to the width) < c (related to the length), or a model for polydisperse unilamellar vesicles with weight-averaged radius $\langle R\rangle$, relative standard deviation $\sigma_R/\langle R\rangle$ and half bilayer thickness ξ, or a model for coexisting micelles and vesicles. All spatial dimensions are given in angstroms (Å). At [SDS]:[DDAB] = 90:10 additional amounts of bilayer sheets are always present which have been modeled as finite circular bilayers with radius R_b ([SDS] + [DDAB] ≤ 0.2 wt %) or infinitely large bilayers. The thickness of the bilayers were assumed to be same as for the coexisting vesicles. The fraction of bilayers and vesicles was too small to accurately determine ξ for the samples $C_{surf}^{tot} = 1.6$ and 2.6 wt % at $X = 0.90$. The structure factor necessary for fitting the data accounts for the comparatively large double layer interactions between macroions with an effective charge z_{eff}. The ideal charge, z_{id}, is the charge of a micelle for which the counterions are fully dissociated. In the samples where micelles and vesicles coexist the influence of interactions for the aggregate in deficit could not be determined, and hence, the corresponding z_{eff} is not given. The fraction of aggregates coexisting with other kinds of aggregates are given in mass % of aggregated surfactant assuming the composition to be identical in the various aggregate structures. The absolute intensities are only accurate within 10%, which means an error of the calculated values of c_{free} of 0.4 mM for the samples at 0.1 wt %, 0.6 mM at 0.15 wt %, 0.8 mM at 0.2 wt %, 1 mM at 0.3 wt %, 2 mM at 0.5 wt %, 2.5 mM at 0.7 wt %, 4 mM at 1.0 wt %, 6 mM at 1.5 wt %, 10 mM at 2.5 wt %, and 20 mM at 5 wt %. The mole fraction x of SDS in the aggregates was calculated from c_{free} assuming only SDS to exist as free monomers.

and below contain only small unilamellar vesicles. The change of composition in the aggregates due to the free monomer effect is also seen from the fact that the relative effective charge of the micelles decreases monotonically from $z_{eff}/z_{id} = 0.32$ at

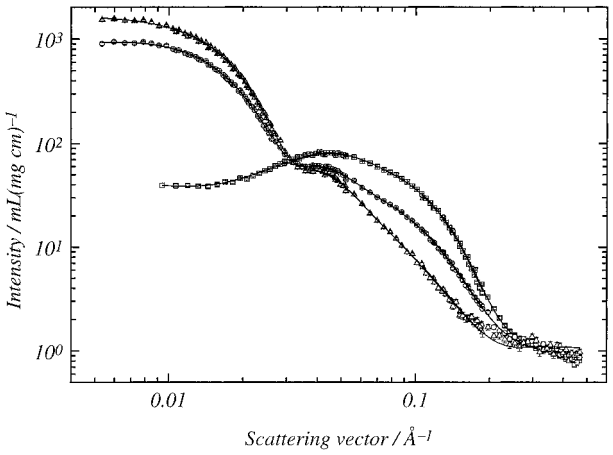

Figure 3. Normalized scattering intensity as a function of the scattering vector q for samples with an overall surfactant concentration [SDS] + [DDAB] = 0.20 wt % (triangular symbols), 0.31 wt % (circular symbols), and 0.72 wt % (squared symbols), respectively, at a given surfactant molar ratio [SDS]:[DDAB] = 95:5. Individual symbols represent SANS data obtained with different combinations of neutron wavelength and sample−detector distance. The lines are the fits with a model for spherical bilayer shells (vesicles, triangles), a model for triaxial ellipsoids (micelles, squares), and a model for coexisting micelles and vesicles (circles). The results of the model fits are given in Table 1. The agreements of the fits as measured by χ^2 are 4.0 (triangles), 1.6 (circles), and 2.2 (squares), respectively.

$c_{surf}^{tot} = 5$ wt % to $z_{eff}/z_{id} = 0.16$ at $c_{surf}^{tot} = 0.5$ wt %. Here, z_{eff} is the effective charge as obtained from our model fits using the RMSA structure factor, and z_{id} is the charge of an aggregate for which the counterions are fully dissociated. SANS data that illustrate the transition from micelles to vesicles when a sample is diluted at fixed $X = 0.95$ are given in Figure 3, together with the model fits that best agree with the data.

The aggregation number N of a surfactant aggregate may be calculated from the aggregate volumes as obtained from the fit parameters and the molecular volumes of the surfactants. Similarly, an apparent aggregation number, N_{app}, may be calculated from the molar weight of the aggregates, as obtained from the absolute intensities, and the molecular weights of the surfactants. It appears that the resulting values of N_{app} are virtually independent of whether counterions or hydrated water molecules are included or not in the surfactant molecular weights. This is because a change in aggregate molar weight, as a result of a varying excess scattering length density of the surfactants, when contributions from counterions and solvent molecules are added corresponds to a similarly large change in the surfactant molecular weights.

When N_{app} is compared with N, it is evident that the amount of aggregated surfactant contributing to the scattering intensity is substantially less than the amount of added surfactant. The reason for this is that a certain amount of surfactants coexists with the micelles as free monomers. Hence, the free monomer concentrations $c_{free} = (1 - N_{app}/N)C_{surf}^{tot}$ may be calculated from the difference between N_{app} and N (values are included in Table 1). In the calculations of N it was assumed, in accordance with arguments given above, that only the hydrocarbon C_{12} tail ($v = 351$ Å^3) of SDS contributes to the scattering intensity, whereas, in addition to the two C_{12} chains of DDAB, also the DA^+ headgroup ($v = 77$ Å^3) contributes to the corresponding quantity of DDAB. If a small part of the diffuse double layer outside the hydrocarbon/water interface of the surfactants was assumed to contribute as well to the scattering intensity, which is a quite reasonable assumption, the calculated values of N would become somewhat smaller, and hence, c_{free} would become somewhat lower than the values given in Table 1. Moreover, the trend of increasing c_{free} with overall surfactant concentration C_{surf}^{tot} observed in Table 1 may also be a result of a too high estimate of N. However, since it is was not possible to employ a two-shell model in order to determine the thickness and composition of such an outer aqueous layer, we have simply omitted it when calculating c_{free}. In addition, the expected 10% error on the absolute intensity implies comparatively large errors of c_{free}. When micelles were seen to coexist with vesicles/lamellae, we have given the mean values of c_{free}, weighted with respect to the fraction of each aggregate, of the corresponding values calculated from the aggregation numbers of micelles and vesicles/lamellae, respectively.

In Table 1 the mole fraction of SDS in the aggregates, as calculated from the values of c_{free} assuming the whole amount of free monomers to be exclusively SDS, has also been included. The assumption is very reasonable considering that SDS (the surfactant in excess) carries the charge in the aggregates and that pure DDAB is insoluble in water. The calculated values of x were used to recalculate c_{free} and x in an iterative way until the two parameters converged. Since c_{free} is determined by the ratio N_{app}/N rather than the absolute values of the two aggregation numbers, the free monomer concentration appears to be rather independent of the assumed composition in the aggregates and, hence, the values of c_{free} and x converge rapidly. From the obtained values of x it is seen that the fraction of SDS in the aggregates increases with c_{surf}^{tot} for a given value of X, in accordance with the arguments given already above in the Introduction. This change in aggregate composition is the reason for the observed transition from micelles to vesicles upon diluting the samples. Due to the uncertainty in absolute intensity, the errors of x are rather large at the lowest surfactant concentrations when the concentration of aggregated SDS is of the same order of magnitude as the error of c_{free}, i.e., at $X = 0.95$ and $c_{surf}^{tot} = 0.1$ wt %, x may vary between $0 < x < 0.8$, and at $X = 0.90$ and $c_{surf}^{tot} = 0.1$ wt % the corresponding values are $0.55 < x < 0.75$. As the concentration of aggregated SDS becomes increasingly larger than the error of c_{free} with increasing surfactant concentration, the errors of x rapidly decrease to become $\sigma(x) = \pm 0.01$ at the highest surfactant concentrations measured.

Also at $X = 0.90$ a transition from micelles to vesicles was observed when the samples were diluted at fixed composition. However, the corresponding data could only be fitted by assuming that a substantial part of bilayers coexist with either micelles or vesicles or both (cf. Figure 4). At low surfactant concentrations about 50% of the mass is in lamellar sheets that coexist with small unilamellar vesicles. Above about $c_{surf}^{tot} = 0.5$ wt %, micelles are the predominating aggregate form, but certain amounts of vesicles and lamellar sheets always coexist with the micelles. At $c_{surf}^{tot} = 5\%$ the solution has separated into one isotropic and one lamellar phase. The isotropic phase was measured and contains a mixture with 20% of the mass in vesicles and 80% mass in the micelles (cf. Figure 5). We obtained radii of the planar bilayer fragments in the range 390 Å $< R_b <$ 470 Å for $c_{surf}^{tot} \leq 0.2$ wt %, whereas the bilayers were too large for their size to be determined from our SANS data at higher surfactant concentrations.

We may note that, as the number of parameters in the model fits strongly increases with the number of different coexisting structures, the various fit parameters become more correlated with each other and, as a result, the error bars are generally larger in these more complex samples. Hence, $\sigma(a) = \pm 0.5$ Å,

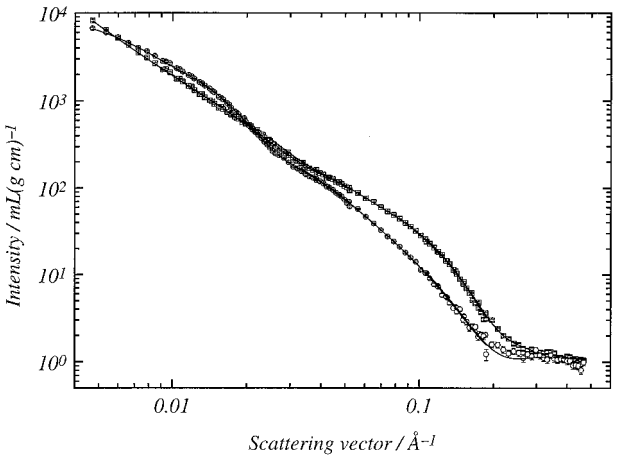

Figure 4. Normalized scattering intensity as a function of the scattering vector q for samples with an overall surfactant concentration [SDS] + [DDAB] = 0.16 wt % (circular symbols) and 0.53 wt % (squared symbols) at a given surfactant molar ratio [SDS]:[DDAB] = 90:10. Individual symbols represent SANS data obtained with different combinations of neutron wavelength and sample−detector distance. The lines are the fits with a model for spherical vesicles coexisting with bilayer fragments (circles) and a model for triaxial ellipsoidal micelles coexisting with vesicles and bilayer fragments (squares). The results from the model fits are given in Table 1. The agreements of the fit as measured by χ^2 are 1.8 (circles) and 3.5 (squares).

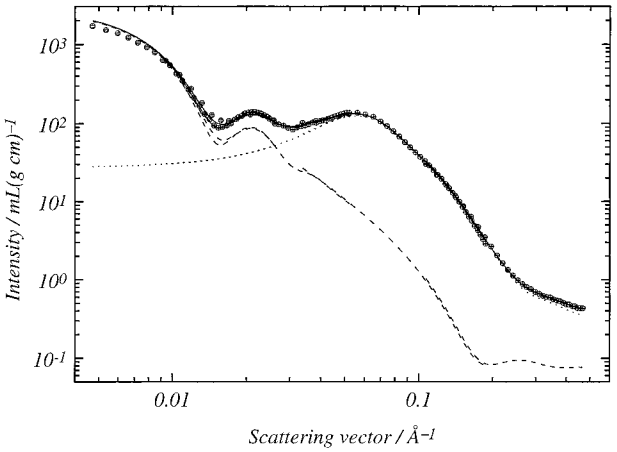

Figure 5. Normalized scattering intensity as a function of the scattering vector q for the isotropic phase (coexisting with a lamellar phase) of the sample with an overall surfactant concentration [SDS] + [DDAB] = 5.3 wt % at a surfactant molar ratio [SDS]:[DDAB] = 90:10. Individual symbols represent SANS data obtained with different combinations of neutron wavelength and sample−detector distance. The lines are the fits with a model for spherical vesicles coexisting with triaxial ellipsoidal micelles. The results from the model fit are given in Table 1. The agreement of the fit as measured by χ^2 is 16.5. The contribution from vesicles to the overall scattering intensity is represented by the dashed line and the contribution from micelles by the dotted line.

$\sigma(b) = \pm 1.5$ Å, and $\sigma(c) = \pm 2$ Å for micelles coexisting with bilayers. The errors for the half bilayer thickness were seen to be typically $\sigma(\xi) = \pm 0.2$ Å for samples where only bilayer structures exist and $\sigma(\xi) = \pm 0.5-1$ Å, depending on vesicle fraction, in samples where micelles and bilayers coexist. For the samples $C_{surf}^{tot} = 1.6$ and 2.6 wt % at $X = 0.90$, the fraction of bilayers was too small for accurate values of ξ to be determined.

The micelles formed at $X = 0.90$ were seen to be slightly larger than at $X = 0.95$, which is consistent with a decreasing surface charge density of the micelles as equimolar composition is approached. The half-axis related to the thickness of the micelles were seen to increase with surfactant concentration from about $a = 13$ Å at $c_{surf}^{tot} = 0.5$ wt % to about 16 Å at $c_{surf}^{tot} = 2.5$ wt % at $X = 0.90$ (cf. Table 1). This may be a consequence of an increasing amount of DDAB in the micelles as the fraction of various bilayer structures (vesicles and lamellar sheets in which DDAB is enriched) was seen to dramatically decrease with increasing c_{surf}^{tot}. The reason for an apparent increase in aggregate thickness with increasing fraction of DDAB is most probably due to the higher scattering contrast for the largely hydrophobic TAB^+ headgroup of DDAB as compared with the sulfate headgroup of SDS. An increasing fraction of DDAB in the micelles probably also accounts for the more pronounced increase in micelle length at $X = 0.90$, as compared with $X = 0.95$, from $c = 27$ Å at $C_{surf}^{tot} = 0.5$ wt % to $c = 57$ Å at $C_{surf}^{tot} = 5$ wt %.

The vesicles formed in dilute mixtures of SDS and DDAB appear to be conspicuously small, i.e. 80 Å $< \langle R \rangle <$ 120 Å, where $\langle R \rangle$ is the number-averaged radial distance from the center to the vesicle bilayer midplane, as compared with what has been found in most other vesicle-forming systems. For example, we have recently studied mixed SDS/DTAB vesicles, and they were never seen to be smaller than $\langle R \rangle = 350$ Å.[9] Vesicles are expected to decrease in size with decreasing work of bending a bilayer into a geometrically closed vesicle.[28] Moreover, geometrical packing constraints account for a large positive contribution to the work of bending a planar bilayer into a vesicle which may be brought down to values where rather small unilamellar vesicles are able to form by several other contributions.[29,30] It was shown that a large negative contribution to the bending work of mixed vesicles due to the asymmetry with respect to the electrostatic free energy contribution, i.e., the difference in charge number, between the two surfactants mixed in a vesicle bilayer is the most important of these (negative) contributions, and hence, unlike the case of micelles (cf. above), mixing has a large tendency to decrease the size of vesicles. An additional asymmetry due to the difference in hydrocarbon tail volumes between SDS and DDAB, as compared with SDS and DTAB, is expected to enhance this effect for SDS-rich vesicles and further bring down the bilayer bending work and, consequently, the size of the vesicles.[31] Above about $c_{surf}^{tot} = 0.7$ wt % at $X = 0.90$ the vesicles become much larger, i.e. $\langle R \rangle \approx 200$ Å, indicating that the composition in the vesicles abruptly changes toward a higher DDAB fraction at this surfactant concentration.

Small vesicles with a size on the same order of magnitude as we have observed for SDS/DDAB have been observed in mixtures of lecithin and bile salts.[32−37] However, when an increasing amount of bile salt is aggregated very long cylindrical wormlike micelles tend to form rather than the much smaller micelles we have observed in mixtures of SDS and DDAB in the absence of added salt.

The size of the vesicles formed at $X = 0.95$ increases from $\langle R \rangle = 88$ Å at $c_{surf}^{tot} = 0.2$ wt % to 109 Å at $c_{surf}^{tot} = 0.1$ wt %, indicating that the bilayer bending work increases with increasing fraction of DDAB in the vesicles (cf. Figure 6). This trend is in qualitative agreement with theoretical calculations of the bending work of bilayers mixed by an anionic and a cationic surfactant.[30] The polydispersity is observed to be rather constant, with a relative standard deviation based on the number-weighted size distribution $0.2 < \sigma_R/\langle R \rangle < 0.3$. This value is somewhat smaller than what was found for the considerably larger SDS/DTAB vesicles ($0.25 < \sigma_R/\langle R \rangle < 0.45$)[9] and may be a result of an increasing significance of third and higher order bending

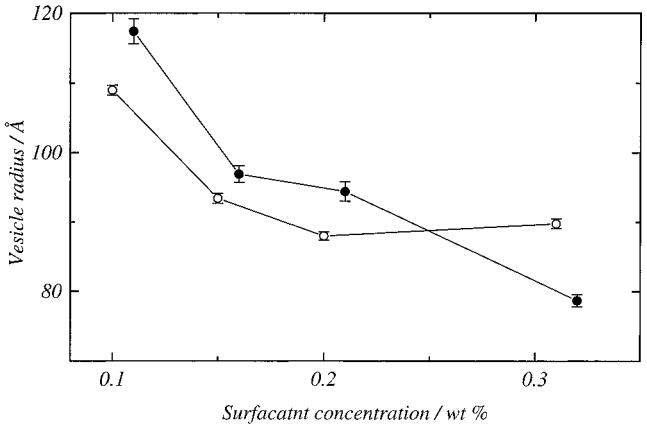

Figure 6. The number-averaged vesicle radius $\langle R \rangle$, with error bars, plotted against the overall surfactant composition $C_{surf}^{tot} \equiv$ [SDS] + [DDAB] at [SDS]:[DDAB] = 95:5 (open symbols) and [SDS]:[DDAB] = 90:10 (solid symbols). The error bars of $\langle R \rangle$ are slightly larger for the more complex samples at [SDS]:[DDAB] = 90:10, as the vesicle radius becomes somewhat correlated with the bilayer radius.

terms to the vesicle free energy as the size of the vesicles is smaller. Half the bilayer thickness was seen to increase at both $X = 0.90$ and 0.95 from about $\xi = 12$ Å at $c_{surf}^{tot} = 0.3$ wt % to $\xi = 14$ Å at $c_{surf}^{tot} = 0.1$ wt %. This is most probably due to an increasing fraction of DDAB in the vesicles with decreasing c_{surf}^{tot} as a result of the free monomer effect discussed above.

The half-axis related to the thickness of the micelles as well as half the thickness of the various bilayer structures was seen to vary between 70 and 100% of a fully extended C_{12} hydrocarbon chain (=16.7 Å). The thickness of micelles as well as bilayers was somewhat larger for the samples at $X = 0.90$, which is consistent with a larger fraction of DDAB in aggregates formed at this composition (cf. Table 1).

In many aspects our results agree very well with what has recently been found by Marques et al., mainly with CRYO-TEM.[14] However, since these authors investigated aqueous mixtures of SDS and DDAB at 25 °C rather than at 38 °C, a perfect agreement with our SANS results cannot be expected. Moreover, the fact that we have used D_2O rather than H_2O as a solvent might also influence the quantitative outcome of our results. A transition from spheroidal micelles to unilamellar vesicles, similar to the one we observed at $X = 0.95$, when a sample is diluted below about 1 wt % at $X = 0.94$ was found by these authors. Moreover, the order of magnitude of the size of micelles as well as vesicles agrees very well with what we have obtained. However, we could not observe any large vesicles (100−200 nm) coexisting with the much smaller ones as was found in the most diluted samples (∼0.1 wt %) in the CRYO-TEM study. The lamellar sheets we observed in the samples at $X = 0.90$ probably correspond to the disklike aggregates, with a length of the edge-on projections of about 50 nm, reported to coexist with vesicles at $0.78 < X < 0.87$. In the most diluted samples we found these bilayers to be about 80−100 nm in diameter, whereas their size became too large for us to determine at higher surfactant concentrations (cf. Table 1). The appearance of a lamellar phase coexisting with the isotropic solution occurred at a slightly higher surfactant concentration (>2.5 wt % at $X = 0.90$) in our study as compared with what was found in ref 14 (>1.0 wt %).

We may finally note that CRYO-TEM is complementary to scattering methods in the sense that the former is used ex situ and the information is measured in direct space, whereas scattering is in situ but in reciprocal space. It is hardly possible to obtain quantitative results of the quality given in Table 1 using electron microscopy. However, since the choice of models used in the analyses of our SANS data agrees very well with the structures found with CRYO-TEM, we think that the latter study excellently confirms the various SANS results presented in Table 1.

Conclusions

It is interesting to compare our SANS results of the structure of rather small anisotropic micelles and unilamellar vesicles formed in mixtures of a single-chain anionic surfactant (SDS) and a double-chain cationic surfactant (DDAB) with our previous results of micelles[8] and vesicles[9] formed in aqueous mixtures of SDS and the oppositely charged single-chain surfactant DTAB, with an almost identical headgroup as DDAB. The transition from micelles, that predominate above about $C_{surf}^{tot} = 0.5$ wt %, to unilamellar vesicles when diluting a sample at fixed surfactant composition X as a result of a free monomer effect was observed in both systems. However, slight differences in the structure of the mixed micelles as well as of the vesicles are found when the two cases are compared.

Mixed tablet-shaped SDS/DTAB micelles at $X = 0.95$ and 40 °C, using 0.1 M NaBr as a solvent, were seen to be almost disk-shaped with the half-axes related to width and length (about 25−26 Å) differing by <1 Å from each other. Mixed SDS/DDAB of similar size (38 °C in the absence of added salt) were, however, seen to be somewhat more elongated, i.e. the half-axes related to the width was $b \approx 23$ Å and the half-axis related to the length of the micelles $c \approx 27$ Å. The vesicles formed in SDS-rich SDS/DDAB samples are considerably smaller (80 Å $< \langle R \rangle <$ 120 Å) than vesicles formed in mixtures of SDS and DTAB (350 Å $< \langle R \rangle <$ 560 Å).

The formation of more elongated micelles as well as considerably smaller unilamellar vesicles in SDS-rich samples of SDS and DDAB can be qualitatively rationalized as being the result of the larger asymmetry between SDS and DDAB as compared with SDS and DTAB. In accordance, an additional contribution to the curvature free energy of micelles and vesicles as a result of the difference in volume of the hydrocarbon parts of SDS and DDAB is expected to give more elongated SDS-rich mixed SDS/DDAB micelles, whereas SDS-rich SDS/DDAB unilamellar vesicles are expected to become smaller as compared with the corresponding SDS/DTAB aggregates. Although these observed differences between mixed SDS/DTAB and SDS/DDAB surfactant aggregates may be qualitatively rationalized, we find it essential to perform quantitative calculations of the curvature free energies of tablet-shaped micelles as well as of unilamellar vesicles.

Acknowledgment. M.B. was supported by a Marie Curie Fellowship from the Training and Mobility of the Researches (TMR) Program of the European Union and by the Center for Surfactants Based on Natural Products (SNAP).

References and Notes

(1) Kaler, E. W.; Herrington, K. L.; Murthy, A. K.; Zasadzinski, J. A. N. *J. Phys. Chem.* **1992**, *96*, 6698.
(2) Kamenka, N.; Chorro, M.; Talmon, Y.; Zana, R. *Colloids Surf.* **1992**, *67*, 213.
(3) Herrington, K. L.; Kaler, E. W.; Miller, D. D.; Zasadzinski, J. A. N.; Chiruvolu, S. *J. Phys. Chem.* **1993**, *97*, 13792.
(4) Yaacob, I. I.; Bose, A. *J. Colloid Interface Sci.* **1996**, *178*, 638.
(5) Talhout, R.; Engberts, J. B. F. N. *Langmuir* **1997**, *13*, 5001.
(6) Bergström, M.; Pedersen, J. S. *Langmuir* **1998**, *14*, 3754.
(7) Bergström, M.; Pedersen, J. S. *Langmuir* **1999**, *15*, 2250.
(8) Bergström, M.; Pedersen, J. S. *J. Phys. Chem. B* **1999**, *103*, 8502.

(9) Bergström, M.; Pedersen, J. S.; Schurtenberger, P. Egelhaaf, S. U. *J. Phys. Chem. B* **1999**, *103*, 9888.
(10) Bergström, M.; Pedersen, J. S. *Phys. Chem. Chem. Phys.* **1999**, *1*, 4437.
(11) Bergström, M. *Langmuir*. Submitted.
(12) Villeneuve, M.; Kaneshina, S.; Imae, T.; Aratono, M *Langmuir* **1999**, *15*, 2029.
(13) Marques, E.; Khan, A.; de Graça Miguel, M.; Lindman, B. *J. Phys. Chem.* **1993**, *97*, 4729.
(14) Marques, E. F.; Regev, O.; Khan, A.; de Graça Miguel, M.; Lindman, B. *J. Phys. Chem. B* **1998**, *102*, 6746.
(15) Marques, E. F.; Regev, O.; Khan, A.; da Graça Miguel, M.; Lindman, B. *J. Phys. Chem. B* **1999**, *103*, 8353.
(16) Pedersen, J. S. *J. Phys. IV (Paris) Coll. C8* **1993**, *3*, 491.
(17) Cotton, J. P. *Neutron, X.-Ray and Light Scattering: Introduction to an Investigative Tool For Colloidal and Polymeric Systems*; Lindner, P., Zemb, T., Eds.; North-Holland: Amsterdam, 1991.
(18) Wignall, G. D.; Bates, F. S. *J. Appl. Crystallogr.* **1986**, *20*, 28.
(19) Chevalier, Y.; Zemb, T. *Rep. Prog. Phys.* **1990**, *53*, 279.
(20) Pedersen, J. S.; Posselt, D.; Mortensen, K. *J. Appl. Crystallogr.* **1990**, *23*, 321.
(21) Bevington, B. R. *Data Reduction and Error Analysis for Physical Sciences*; McGraw-Hill: New York, 1969.
(22) Pedersen, J. S. *Adv. Colloid Interface Sci.* **1997**, *70*, 171.
(23) Kotlarchyk, M.; Chen, S. H. *J. Chem. Phys.* **1983**, *79*, 2461.
(24) Hayter, J. B.; Penfold, J. *Mol. Phys.* **1981**, *42*, 409.
(25) Hansen, J. P.; Hayter, J. B. *Mol. Phys.* **1982**, *46*, 651.
(26) Mittelbach, P.; Porod, G. *Acta Phys. Austriaca* **1962**, *15*, 122.
(27) Bergström, M. *J. Chem. Phys.*, submitted.
(28) Bergström, M.; Eriksson, J. C. *Langmuir* **1998**, *14*, 288.
(29) Bergström, M.; Eriksson, J. C. *Langmuir* **1996**, *12*, 624.
(30) Bergström, M. *Langmuir* **1996**, *12*, 2454.
(31) Bergström, M. Unpublished.
(32) Hjelm, R. P.; Thiyagarajan, P.; Alkan, H. *J. Appl. Crystallogr.* **1988**, *21*, 858.
(33) Hjelm, R. P.; Alkan, H.; Thiyagarajan, P. *Mol. Cryst. Liq. Cryst.* **1990**, *180A*, 155.
(34) Hjelm, R. P.; Thiyagarajan, P.; Sivia, D. S.; Lindner, P.; Alkan, H.; Schwahn, D. *Prog. Colloid Polym. Sci.* **1990**, *81*, 225.
(35) Hjelm, R. P.; Thiyagarajan, P.; Alkan, H. *J. Phys. Chem.* **1992**, *96*, 8653.
(36) Long, M. A.; Kaler, E. W.; Lee, S. P.; Wignall, G. D. *J. Phys. Chem.* **1994**, *98*, 4402.
(37) Pedersen, J. S.; Egelhaaf, S. U.; Scurtenberger, P. *J. Phys. Chem.* **1995**, *99*, 1299.